

Orbital-driven melting of a bosonic Mott insulator in a shaken optical lattice

Christoph Sträter* and André Eckardt†

Max-Planck-Institut für Physik komplexer Systeme, Nöthnitzer Straße 38, 01187 Dresden, Germany

(Dated: April 17, 2015)

In order to study the interesting interplay between localized and dispersive orbital states in a system of strongly interacting ultracold atoms in an optical lattice, we investigate the possibility to coherently couple the lowest two Bloch bands by means of resonant periodic forcing. For bosons in one dimension we show that a strongly interacting Floquet system can be realized, where at every lattice site two (and only two) near-degenerate orbital states are relevant, whose tunneling matrix elements differ in sign and magnitude. By smoothly tuning both states into resonance, the system is predicted to undergo an orbital-driven Mott-insulator-to-superfluid transition. As a consequence of kinetic frustration, this transition can be either continuous or first-order, depending on parameters such as lattice depth and filling.

PACS numbers: 37.10.Jk, 03.75.Lm, 67.85.-d, 75.30.Mb

I. INTRODUCTION

Orbital degrees of freedom play an important role in solid-state systems. A prominent example is the intriguing physics of heavy-fermion compounds that emerges from the interplay between dispersive conduction-band orbitals on the one hand and strongly localized orbitals, with a large effective mass and strong Coulomb interactions, on the other [1–4]. However, in systems of ultracold atoms in optical lattices [5, 6] orbital degrees of freedom, spanning Bloch bands above a large energy gap, are typically frozen out, at least in the interesting deep-lattice tight-binding regime where interactions are strong. Here, we investigate the possibility to coherently open on-site orbital degrees of freedom in a strongly interacting optical lattice system by means of near-resonant lattice shaking. We consider spinless bosons in one dimension (1D) and show how to realize a “dressed-lattice” system, where effectively at every lattice site the strongly localized ground-band orbital is nearly degenerate and coupled to the much more dispersive first-excited-band orbital. The tunneling matrix elements of the two orbitals differ strongly in magnitude and also in sign, with the latter leading to kinetic frustration. We predict an orbital-driven phase transition between a Mott insulator (MI) and a superfluid (SF) state when the population of the light orbitals is adiabatically increased by lowering the interorbital detuning. As a consequence of frustration and strong interorbital interactions, this transition is found to be either continuous or first-order, depending on parameters such as filling or lattice depth.

In contrast to the present proposal, in previous experiments atoms were transferred non-adiabatically to excited bands of optical lattices by different methods [7–12]. Moreover, lattice shaking has recently been employed for band-coupling in the weakly interacting regime, where condensation into two possible momentum states led to domain formation [13]. Such band-coupling has been studied theoretically for non/weakly interacting particles

and isolated sites [14–20]. Also orbital coupling via magnetic resonances has been proposed [21] and there has been theoretical interest in the physics of excited orbitals not involving lower-lying states [22–28]. Finally, the perturbative admixture of excited orbitals has been studied in theory [29–36] and experiment [37–42].

II. REALIZING THE TWO-ORBITAL MODEL

Consider spinless bosonic atoms of mass m in an optical lattice $V(\mathbf{r}) = V_0 \sin^2(k_L x) - V_1 \sin^2(2k_L x) + V_\perp [\sin^2(k_L y) + \sin^2(k_L z)]$. The y and z directions are frozen out by a deep lattice, we will assume $V_\perp = 30E_R$, such that an array of 1D tubes with a dimerized lattice [Fig. 1(a)] is created. The recoil energy $E_R = \hbar^2 k_L^2 / 2m$ is needed to localize a particle on a lattice constant π/k_L . For Rb^{87} a typical wave length of $2\pi/k_L = 852 \text{ nm}$ gives $E_R = 2\pi\hbar \cdot 3.16 \text{ kHz}$. Each 1D tube is described by the multi-band Bose-Hubbard Hamiltonian $\hat{H}_0 = \hat{H}_{\text{kin}} + \hat{H}_{\text{os}}$, where

$$\hat{H}_{\text{kin}} = - \sum_{\ell} \sum_{\alpha} (-1)^{\alpha} J_{\alpha} (\hat{b}_{\alpha(\ell+1)}^{\dagger} \hat{b}_{\alpha\ell} + \text{h.c.}), \quad (1)$$

$$\hat{H}_{\text{os}} = \sum_{\ell} \left[\sum_{\alpha} \epsilon_{\alpha} \hat{n}_{\alpha\ell} + \sum_{\{\alpha\}} \frac{U_{\{\alpha\}}}{2} \hat{b}_{\alpha_1\ell}^{\dagger} \hat{b}_{\alpha_2\ell}^{\dagger} \hat{b}_{\alpha_3\ell} \hat{b}_{\alpha_4\ell} \right] \quad (2)$$

Here $\hat{b}_{\alpha\ell}^{\dagger}$ and $\hat{n}_{\alpha\ell}$ are the bosonic creation and number operator for a Wannier orbital $w_{\alpha}(x - x_{\ell})$ of Bloch band $\alpha = 0, 1, \dots$, localized at $x_{\ell} = \ell\pi/k_L$ [43]. The band-center energies and tunnel parameters fulfill $0 \equiv \epsilon_0 < \epsilon_1 < \dots$ and $0 < J_0 < J_1 < \dots$, respectively. The interaction strengths $U_{\{\alpha\}} \equiv U_{\alpha_1\alpha_2\alpha_3\alpha_4} = (2\hbar^2 a_s^2 / m) \int dx w_{\alpha_1}(x) w_{\alpha_2}(x) w_{\alpha_3}(x) w_{\alpha_4}(x)$ vanish for odd $\sum_i \alpha_i$, since $w_{\alpha}(x) = (-)^{\alpha} w_{\alpha}(-x)$, and depend on the transverse localization length $a_{\perp} \simeq (V_{\perp}/E_R)^{1/4}/k_L$ and the scattering length a_s ($\approx 5.6 \text{ nm}$ for Rb^{87}).

In the tight-binding regime, ϵ_1 is typically much larger than the temperature and the chemical potential so that the orbital degree of freedom α is frozen out. We wish to

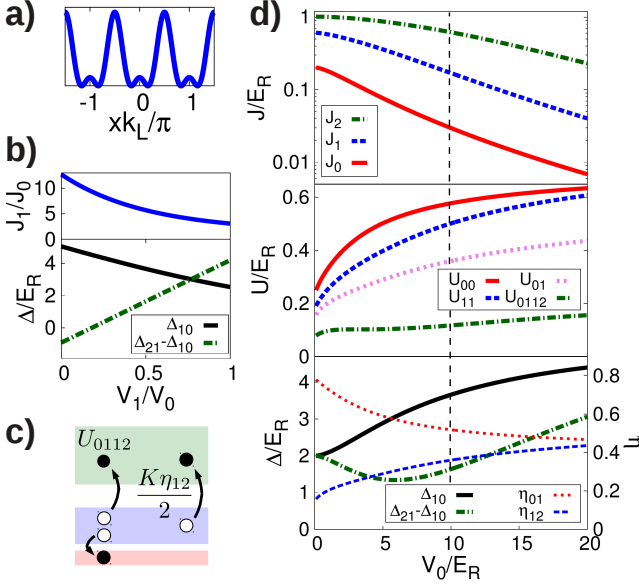


FIG. 1. (color online) (a) Dimerized lattice with $V_1/V_0 = 0.5$. (b) Impact of V_1/V_0 on J_2/J_1 , Δ_{10} , and Δ_{21} , for $V_0/E_R = 10$. (c) Most dominant loss channels, scattering into third band (zero-photon process) and driving-induced coupling (single-photon process), are off-resonant due to dimerization. (d) Lattice parameters versus V_0/E_R for $V_1/V_0 = 0.5$ and Rb⁸⁷.

coherently open this freedom by means of time periodic forcing with near-resonant frequency $\hbar\omega \approx \epsilon_1$. In particular, the lowest band ($\alpha = 0$) shall be coupled to the more dispersive first excited band ($\alpha = 1$), without creating coupling to even higher-lying bands ($\alpha \geq 2$). In order to achieve such a controlled situation—also in the regime where interactions are strong compared to tunneling—we combine two strategies: First we choose a driving scheme, namely sinusoidally shaking the lattice back and forth, that for weak forcing does not lead to multi-“photon” interband transitions at resonances $\Delta_{\alpha'\alpha} \equiv \epsilon_{\alpha'} - \epsilon_\alpha \approx m\hbar\omega$ with integer $|m| \geq 2$. Second, we engineer the band structure by varying V_1/V_0 such that transitions to band 2 remain off resonant: With increasing V_1/V_0 the bands organize in pairs (0,1), (2,3), ... such that Δ_{10} and Δ_{32} as well as J_1/J_0 and J_3/J_2 decrease, while Δ_{21} increases. For $V_0 = 10E_R$, already a slight dimerization $V_1/V_0 = 0.5$ ensures that $\Delta_{10} \approx 3.7E_R$ is noticeably smaller than $\Delta_{21} \approx 5.3E_R$, rendering the Δ_{21} transition off-resonant when $\hbar\omega \approx \Delta_{10} = \epsilon_1$. At the same time $V_1/V_0 = 0.5$ is small enough to keep a relatively large ratio $J_1/J_0 \approx 5.7$, retaining the desired feature that $\alpha = 0$ particles are much less dispersive than $\alpha = 1$ particles [Fig. 1(b,d)].

By moving the lattice like $Kk_L/(\pi m\omega^2) \cos(\omega t)$ in x direction, an inertial force is created, described by

$$\hat{H}_{\text{dr}}(t) = K \cos(\omega t) \sum_{\ell} \left[\sum_{\alpha} \ell \hat{n}_{\alpha\ell} + \sum_{\alpha'\alpha} \eta_{\alpha'\alpha} \hat{b}_{\alpha'\ell}^{\dagger} \hat{b}_{\alpha\ell} \right]. \quad (3)$$

Here $\eta_{\alpha'\alpha} = (k_L/\pi) \int dx w_{\alpha'}(x) x w_{\alpha}(x)$ vanishes for even $\alpha' + \alpha$. We employ a time-periodic unitary transformation $\hat{U}(t) = \exp(-i \sum_{\ell,\alpha} \hat{n}_{\alpha\ell} \nu_{\alpha} \omega t)$ with integers ν_{α} , designed to shift all band energies ϵ_{α} to values $\epsilon'_{\alpha} \equiv \epsilon_{\alpha} - \nu_{\alpha} \hbar\omega \in (-\hbar\omega/2, \hbar\omega/2]$ that are as close as possible to $\epsilon_0 = \epsilon'_0 = 0$. This gives $|\epsilon'_1| = |\epsilon_1 - \hbar\omega| \ll \hbar\omega$ by choice of ω and $|\epsilon'_2| = |\epsilon_2 - 2\hbar\omega| \sim \hbar\omega/2$ by choice of V_1/V_0 ; all other ϵ'_{α} are scattered somehow between $-\hbar\omega/2$ and $\hbar\omega/2$. The periodic time dependence of the transformed Hamiltonian $\hat{H}(t) = \hat{U}^{\dagger}(\hat{H}_0 + \hat{H}_{\text{dr}})\hat{U} - i\hbar\hat{U}^{\dagger}d_t\hat{U}$ appears in the interband coupling parameters $K\eta_{\alpha'\alpha} \cos(\omega t)e^{i(\nu_{\alpha'} - \nu_{\alpha})\omega t}$ and $U_{\{\alpha\}}e^{i(\nu_{\alpha_1} + \nu_{\alpha_2} - \nu_{\alpha_3} - \nu_{\alpha_4})\omega t}$. For weak forcing $K \ll \hbar\omega$ the driving frequency $\hbar\omega \sim \Delta_{10}$ is large compared to the intraband terms as well as to the band coupling [Fig. 1(d)]. This allows to average the rapidly oscillating terms in the Hamiltonian over one driving period and to approximately describe the system by the effective time-independent Hamiltonian $\hat{H}_{\text{eff}} = \frac{1}{T} \int_0^T dt \hat{H}(t)$, reading

$$\begin{aligned} \hat{H}_{\text{eff}} = & \hat{H}_{\text{kin}} + \sum_{\ell} \left[\sum_{\alpha} \epsilon'_{\alpha} \hat{n}_{\alpha\ell} + K \sum_{\alpha'\alpha} \eta'_{\alpha'\alpha} \hat{b}_{\alpha'\ell}^{\dagger} \hat{b}_{\alpha\ell} \right. \\ & \left. + \sum_{\{\alpha\}} \frac{U'_{\{\alpha\}}}{2} \hat{b}_{\alpha_1\ell}^{\dagger} \hat{b}_{\alpha_2\ell}^{\dagger} \hat{b}_{\alpha_3\ell} \hat{b}_{\alpha_4\ell} \right], \end{aligned} \quad (4)$$

with $\eta'_{\alpha'\alpha} = \eta_{\alpha'\alpha}(\delta_{\nu_{\alpha'}, \nu_{\alpha}+1} + \delta_{\nu_{\alpha'}, \nu_{\alpha}-1})/2$ and $U'_{\{\alpha\}} = U_{\{\alpha\}}\delta_{\nu_{\alpha_1} + \nu_{\alpha_2}, \nu_{\alpha_3} + \nu_{\alpha_4}}$. For a more systematic derivation of Eq. (4), \hat{H}_{eff} is defined as the generator of the time evolution over one period [44] and computed using degenerate perturbation theory in the extended Floquet Hilbert space [45], similar like in Refs. [46, 47]. In leading order one recovers Eq. (4). The leading correction contains tiny second-order coupling to bands $\alpha \geq 3$ of order $c^2/\hbar\omega$ to be neglected, where $c \lesssim 0.1E_R$ is a typical interband coupling matrix element and $\hbar\omega \gtrsim 3E_R$.

It is a crucial property of lattice shaking (3) that in \hat{H}_{eff} the interband coupling $K\eta'_{\alpha'\alpha}$ is a single-photon process, with $\nu_{\alpha'} = \nu_{\alpha} \pm 1$, and that scattering $U'_{\{\alpha\}}$ is a zero-photon process, with $\nu_{\alpha_1} + \nu_{\alpha_2} = \nu_{\alpha_3} + \nu_{\alpha_4}$. No multi-photon processes are found for weak driving. Thus, in \hat{H}_{eff} above the bands 0 and 1 are coupled to band 2 only, via the processes sketched in Fig. 1(c). These processes are, however, off-resonant, since $\epsilon'_2 \sim \hbar\omega$. The bands 0 and 1 are, therefore, to good approximation isolated and described by the two-band (2B) model

$$\begin{aligned} \hat{H}_{2B} = & \hat{H}_{\text{kin}} + \sum_{\ell} \left[\delta \hat{n}_{1\ell} - \gamma (\hat{b}_{1\ell}^{\dagger} \hat{b}_{0\ell} + \text{h.c.}) + 2U_{10} \hat{n}_{0\ell} \hat{n}_{1\ell} \right. \\ & \left. + \frac{U_{00}}{2} \hat{n}_{0\ell} (\hat{n}_{0\ell} - 1) + \frac{U_{11}}{2} \hat{n}_{1\ell} (\hat{n}_{1\ell} - 1) \right], \end{aligned} \quad (5)$$

where $\gamma = -K\eta_{10}/2$, $U_{\alpha'\alpha} \equiv U_{\alpha\alpha'\alpha'\alpha}$ and $\delta = \Delta_{10} - \omega$. For $V_0 = 10E_R$, $V_1/V_0 = 1/2$, and $K = 0.5E_R$ we obtain $J_0 \approx 0.030E_R$, $J_1 \approx 0.17E_R$, $\gamma \approx 0.13E_R$, $U_{00} \approx 0.58E_R$, $U_{01} \approx 0.36E_R$, and $U_{11} \approx 0.50E_R$.

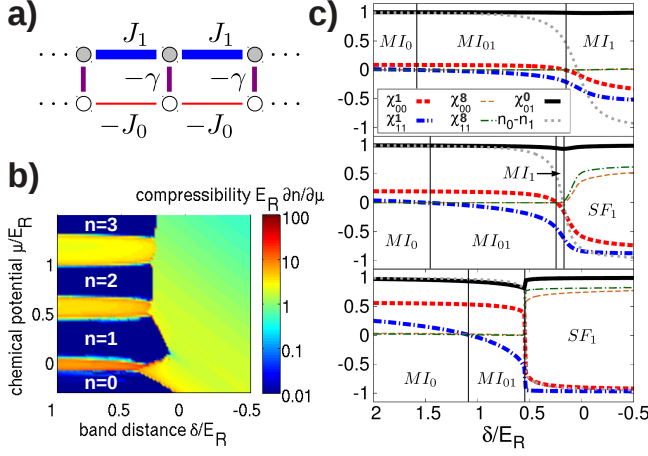


FIG. 2. (color online) (a) Sketch of the effective model, grey (white) circles correspond to the $\alpha = 1$ (0) state at each site ℓ , with energy δ (0). (b) Ground-state compressibility $\partial_\mu n E_R$ in the μ - δ plane for $V_0/E_R = 10$ and $V_1/V_0 = 1/2$. (c) Correlations $\chi_{\alpha'\alpha}^{\ell} \equiv \langle \hat{b}_{\alpha'\ell}^\dagger \hat{b}_{\alpha 0} \rangle / \sqrt{n_{\alpha'} n_{\alpha}}$ and imbalance $n_0 - n_1$ for fixed filling $n = 1$ versus δ , with $V_1/V_0 = 0.5$ and $V_0/E_R = 15, 10, 5$ (from top to bottom). Numerical data in (b) and (c) obtained for $M = 30$ rungs under periodic boundary conditions using TEBD in imaginary time [48, 49], with bond dimensions 14 (b) and 30 (c).

\hat{H}_{2B} describes a highly tunable 1D ladder system [Fig. 2(a)] with interesting properties: The tunneling matrix elements along both legs (i.e. in both bands) differ in sign and magnitude. The former leads to maximal kinetic frustration with a flux of π per plaquette [50–57]. The latter makes leg 0 more prone to localization than leg 1. The hybridization of both legs is controlled by the energy separation δ and the coupling γ , which can be tuned via the frequency and strength of the driving, respectively. Finally, the system features strong interorbital interactions U_{10} , with two-particle energies $2U_{01} > U_{00} > U_{11}$.

In order to investigate the 2B model (5), the following experimental protocol can be pursued. After the system is prepared in (or close to) the undriven ground state, populating band 0, the driving strength K is ramped up smoothly to the desired value. During this step the detuning δ is still large enough to suppress any significant occupation of band 1. Then, the orbital freedom is opened by smoothly lowering δ .

III. ORBITAL-DRIVEN MOTT TRANSITION

We study the ground state of \hat{H}_{2B} versus δ . For large positive (negative) $\delta/|\gamma|$ only leg 0 (leg 1) will be occupied; the system effectively reduces to a 1D Bose-Hubbard chain. For integer filling of n particles per site, the ground state of such a chain with tunneling J and on-site repulsion U is a gapped (i.e. incompressible)

MI with localized particles if $J/U < (J/U)_c^{(n)}$, where $(J/U)_c^{(1)} \approx 0.26$ [58]. Otherwise, it is a gapless SF with quasilinear-range order. Thus, for $n = 1$ the system is a MI for $\delta \gg |\gamma|$, since $J_0/U_{00} \approx 0.051$, and a SF for $-\delta \gg |\gamma|$, since $J_1/U_{11} \approx 0.34$.

It is instructive to control n via the chemical potential μ , introduced by adding $-\mu \sum_{\ell} (\hat{n}_{0\ell} + \hat{n}_{1\ell})$ to \hat{H}_{2B} . In Fig. 2(b), we plot the ground-state compressibility $\partial_\mu n$ in the μ - δ plane, computed by time-evolving block decimation (TEBD) in imaginary time [48, 49]. As expected [58], for $\delta/|\gamma| \gg 1$ we find incompressible MI phases at integer filling n , interrupted by SF phases where n changes in μ direction, while for $-\delta/|\gamma| \gg 1$ the system is a compressible SF. When δ is lowered, the filling n_0 (n_1) of leg 0 (1) decreases (increases). In response, an orbital-driven transition occurs, either between a MI and a SF or, for fractional filling, between different SFs. For the given parameters, these are first-order transitions, except at the tip of the $n = 1$ Mott phase, where a continuous transition is found. The discontinuous SF-to-SF transition, where the ground state changes abruptly, happens when near $\delta = 2(J_0 - J_1) \approx -0.28 E_R$ a boson suddenly prefers to delocalize with quasimomentum π in leg 1, rather than with quasimomentum 0 in leg 0. The discontinuous MI-to-SF transition, to be explained below, is more subtle.

A strong-coupling argument explains the orbital-driven MI-to-SF transition. Within the MI state, n_1 increases smoothly when δ is lowered, and the larger n_1 the larger is the reduction of kinetic energy $\approx 2J_1(n_1 + 1)$ (or $\approx 2J_1 n_1$) that a particle (or a hole) acquires by delocalizing along leg 1 on the MI background. When the kinetic energy reduction of a particle-hole excitation exceed its interaction-energy cost $\approx (U_{11} + 2U_{01}n_0\delta_{n,1})$, these excitations proliferate and the ground state becomes a SF as seen in Fig. 2(b). This transition can also be observed in Fig. 2(c, middle) where we plot $n_0 - n_1$ and the ground-state correlations $\chi_{\alpha'\alpha}^{\ell} \equiv \langle \hat{b}_{\alpha'\ell}^\dagger \hat{b}_{\alpha 0} \rangle / \sqrt{n_{\alpha'} n_{\alpha}}$ versus δ , for the same parameters and sharp filling $n = 1$ [59]. While $|\chi_{\alpha'\alpha}^{\ell}|$ decays exponentially with ℓ in the MI phase, in the SF regime the decay is only algebraic. Therefore, the transition is indicated by a significant increase of correlations on longer distances such as $\chi_{\alpha'\alpha}^8$. It is found near $\delta = 0.2 E_R$, in fair agreement with the above estimate giving $n_0 - n_1 \approx (8J_1 - U_{11} - 2U_{01}) / (4J_1 + 2U_{01}) \approx 0.10$.

In Fig. 2(c, middle) we can identify three different types of MI states, characterized by respective signs $s_{\alpha} \equiv \text{sgn}(\chi_{\alpha'\alpha}^1)$ of the short-range correlations along both legs. This is a consequence of kinetic frustration; while the tunneling matrix elements $-J_0$ and J_1 favor $s_0 = +1$ and $s_1 = -1$, the rung coupling $-\gamma$ favors $s_0 = s_1$. We use the label MI_{01} if both legs retain their favored correlations ($s_0 = -s_1 = +1$), and MI_{α} if leg α dominates the other one [$s_0 = s_1 = +1$ (-1) for $\alpha = 0$ (1)]; similar labels are used for SF states. Due to the strong interleg interactions $2U_{01} > U_{00}, U_{11}$ the system

does not feature the chiral time-reversal symmetry broken MI or SF ground states with complex $\chi_{\alpha'\alpha}^\ell$ predicted in Ref. [56]. Treating both γ and the J_α as perturbation the MI₀-to-MI₀₁ transition is predicted to occur at $\delta = U_{00}J_1/(2J_0) \approx 1.6$ [60]. Experimentally, this transition is hardly observable, since it occurs at tiny $n_1 \simeq |\gamma/\delta|^2 \approx 0.007$. The MI₀₁-to-MI₁, happening when δ is lowered further, is of greater importance. A perturbative treatment of the tunneling matrix elements J_α , neglecting γ and δ on interaction-dominated doubly occupied sites, predicts this transition to occur when $n_0 - n_1 \approx [(J_1 - J_0)U_{00} - 4J_0U_{01}]/[(J_1 - J_0)U_{00} + 4J_0U_{01}] \approx 0.31$ [60], in reasonable agreement with the numerics. These transitions can be observed also in a deeper lattice, where the system remains a MI for small δ [Fig. 2(c,top)].

For a lower lattice depth of $V_0/E_R = 5$, the MI-to-SF transition occurs earlier and already within the MI₀₁ regime [Fig. 2(c,bottom)]. This is explained by the above estimates that predict the MI-to-SF transition to occur when $n_0 - n_1 \approx 0.94$, well before the estimated value $n_0 - n_1 \approx 0.23$ for the MI₀₁-to-MI₁ transition is reached. As a consequence, the MI-to-SF transition is rendered discontinuous. The discontinuity results from an abrupt change in the structure of the short-range correlations along leg 0. Namely, the SF phase is of SF₁ type, with $s_0 = s_1 = -1$, such that the short-range correlations along leg 0 have to undergo a finite jump at the MI₀₁-to-SF₁ transition. The same argument also explains the first-order nature of the orbital-driven MI-to-SF transitions for $V_0/E_R = 10$ at filling $n \geq 2$, visible as a sharp jump of the compressibility in Fig. 2(b). All in all, the fact that the orbital-driven MI-to-SF transition can be discontinuous results from the combination of kinetic frustration, tunneling imbalance $J_1 \gg J_0$, and strong interband interactions U_{01} , all stemming from the spatial structure of the Wannier orbitals.

IV. PREPARATION DYNAMICS AND HEATING

When δ is lowered slow enough, the system is expected to approximately follow the ground state of the 2B model (5), unless the first-order transition is crossed. This desired dynamics is effectively adiabatic [47], i.e. adiabatic with respect to \hat{H}_{2B} , but diabatic with respect to tiny coupling matrix elements neglected in \hat{H}_{2B} . We have simulated the time evolution of the system [Fig. 3(a)] using TEBD [48, 49]. For parameters like in Fig. 2(c,middle), δ/E_R is ramped from 1 to -0.5 within a time $T_r = 500\hbar/E_R \approx 25\text{ms}$. In order to probe the validity of the 2B model (5), we include the major “loss” processes depicted in Fig. 1(c) by employing Hamiltonian (4) with three bands ($\alpha = 0, 1, 2$). In Fig. 3(a), one can clearly see that the $\alpha = 2$ occupation n_2 remains very low and that the overlap with the instantaneous 2B ground state stays close to 1. Both clearly shows that

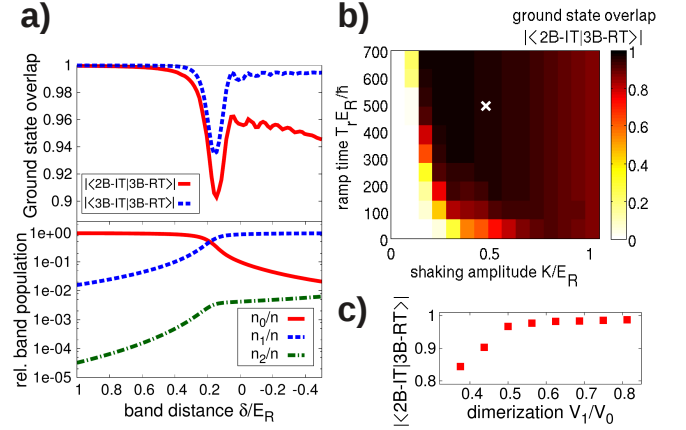


FIG. 3. (color online) Real-time (RT) evolution of the effective model (4) with three bands (3B) $\alpha = 0, 1, 2$, obtained by TEBD [48, 49] with bond dimensions 24 (a), 22 (b), and 22-40 (c). (a) Occupations and overlaps with the [imaginary time-evolved (IT)] ground states of the 3B and 2B model. Starting in the ground state at $\delta = \epsilon_1 - \omega = 1E_R$, δ is lowered linearly to $\delta = -0.5E_R$ within a time of $T_r = 500\hbar/E_R$; for $n = 1$, $V_0/E_R = 10$, $V_1/V_0 = 0.5$, $K/E_R = 0.5$ and $M = 16$ rungs under periodic boundary conditions. (b) After-ramp overlap for $M = 10$, like in (a) but varying T_r and K . (c) After-ramp overlap for $M = 10$, like in (a), but varying V_1/V_0 .

the driving does not cause detrimental heating and justifies a description of the driven system in terms of the 2B model (5). It, moreover, indicates that an effectively adiabatic time evolution is possible, despite a noticeable dip of the overlap at the Mott transition (resembling the behavior of Landau-Zener sweeps [61]). Thus, the protocol allows for the preparation of stable low-entropy states in an excited Bloch band.

The overlap plotted in Fig. 3(b) versus T_r and K measures the effective adiabaticity. Too small T_r and $\gamma \propto K$ spoil the adiabatic dynamics within the 2B model and for too large K the coupling to band 2 becomes relevant. Moreover, for too large K and T_r slow second-order loss processes (not included) can occur. Finally, Fig. 3(c) shows that for strong interactions a minimal dimerization of $V_1/V_0 = 0.5$ is crucial. Different from the weakly interacting case [13], we find significant transfer to the second excited band 2 for the simple cosine lattice ($V_1/V_0 = 0$).

V. CONCLUSION AND OUTLOOK

We have shown that lattice shaking is a feasible tool to coherently open on-site orbital degrees of freedom in a strongly interacting optical lattice system and that the interplay between Wannier orbits of different structure gives rise to rich physics already for spinless bosons in 1D. Extending the scheme to spinful fermions, the interplay between strongly localized and dispersive orbital

states should permit to mimic aspects of the intriguing heavy-fermion physics and to realize periodic-Anderson-like models [1–4]. The extension to higher dimensional lattices should provide a feasible scheme for the preparation of low-entropy states in excited bands as they have been discussed before [22–28] and, moreover, to couple them to strongly localized lowest-band orbits. Finally, by employing sufficiently off resonant forcing, keeping δ large enough, one might enhance and control the perturbative admixtures of excited bands [29–42], e.g. in order to enhance superexchange processes by engineering density-dependent tunneling.

We thank Miklós Gulácsi for discussion. CS is grateful for support by the Studienstiftung des deutschen Volkes.

APPENDIX A: TRANSITION BETWEEN MI_0 AND MI_{01}

For large negative δ , one can treat both γ and the tunneling matrix elements J_α as a perturbation. For unit filling $n = 1$ the unperturbed ground state takes the simple form

$$|\psi_0\rangle = \prod_{\ell} \hat{b}_{0\ell}^\dagger |\text{vac}\rangle \quad (6)$$

with the vacuum state $|\text{vac}\rangle$. A finite correlation $\langle \hat{b}_{10}^\dagger \hat{b}_{11}^\dagger \rangle$ will appear in third order. Namely one has

$$\begin{aligned} \langle \psi | \hat{b}_{10}^\dagger \hat{b}_{11} | \psi \rangle &\simeq \langle \psi_1 | \hat{b}_{10}^\dagger \hat{b}_{11} | \psi_2 \rangle + \langle \psi_2 | \hat{b}_{10}^\dagger \hat{b}_{11} | \psi_1 \rangle \\ &= 2 \langle \psi_1 | \hat{b}_{10}^\dagger \hat{b}_{11} | \psi_2 \rangle \end{aligned} \quad (7)$$

with $|\psi_k\rangle$ denoting the state correction appearing in k th order perturbation theory. Here the relevant term of $|\psi_1\rangle$ reads

$$\frac{-\gamma \hat{b}_{10}^\dagger \hat{b}_{00}}{-\delta} |\psi_0\rangle = \frac{\gamma}{\delta} \hat{b}_{10}^\dagger \prod_{\ell \neq 0} \hat{b}_{0\ell}^\dagger |\text{vac}\rangle, \quad (8)$$

and the relevant term of $|\psi_2\rangle$ takes the form

$$\begin{aligned} &\left(\frac{\gamma \hat{b}_{11}^\dagger \hat{b}_{01} J_0 \hat{b}_{01}^\dagger \hat{b}_{00}}{(2U_{01} + \delta)U_{00}} - \frac{J_1 \hat{b}_{11}^\dagger \hat{b}_{10} \gamma \hat{b}_{10}^\dagger \hat{b}_{00}}{(2U_{01} + \delta)\delta} \right) |\psi_0\rangle \\ &= \left(\frac{2J_0}{U_{00}} - \frac{J_1}{\delta} \right) \frac{\gamma}{2U_{12} + \delta} \hat{b}_{11}^\dagger \prod_{\ell \neq 0} \hat{b}_{0\ell}^\dagger |\text{vac}\rangle. \end{aligned} \quad (9)$$

With that we arrive at

$$\langle \hat{b}_{10}^\dagger \hat{b}_{11}^\dagger \rangle \simeq \left(\frac{2J_0}{U_{00}} - \frac{J_1}{\delta} \right) \frac{2\gamma^2}{(2U_{12} + \delta)\delta} \quad (10)$$

leading to a sign change when both terms in the round bracket cancel each other. The change from positive to negative sign corresponds to the transition from MI_0 to MI_{01} that is thus expected to occur at

$$\delta = \frac{U_{00}J_1}{2J_0}. \quad (11)$$

APPENDIX B: TRANSITION BETWEEN MI_{01} AND MI_1

We assume sharp filling $n = n_0 + n_1 = 1$ and treat the tunnel terms as a perturbation. The unperturbed on-site problem is then given by

$$\begin{aligned} \hat{H}_0 &= \delta \hat{n}_1 - \gamma (\hat{b}_1^\dagger \hat{b}_0 + \hat{b}_0^\dagger \hat{b}_1) + 2U_{01} \hat{n}_0 \hat{n}_1 \\ &\quad + \frac{U_{00}}{2} \hat{n}_0 (\hat{n}_0 - 1) + \frac{U_{11}}{2} \hat{n}_1 (\hat{n}_1 - 1) \end{aligned} \quad (12)$$

where we dropped the site index ℓ . In the subspace of one particle on a site the unperturbed ground state reads

$$|\psi^{(0)}\rangle = (a_0 \hat{b}_0^\dagger + a_1 \hat{b}_1^\dagger) |\text{vac}\rangle, \quad (13)$$

with energy $\varepsilon_0 = \frac{\delta}{2} - \frac{1}{2}[\delta^2 + 4\gamma^2]^{1/2}$ per site and $a_1/a_0 = -\varepsilon_0/\gamma$, with $a_0^2 + a_1^2 = 1$, giving in leading order perturbation theory

$$n_0 \simeq a_0^2 \quad \text{and} \quad n_1 \simeq a_1^2. \quad (14)$$

In the course of the perturbation calculation we also need defect states with one particle less (a hole) and one extra particle. The hole state is simply given by the vacuum

$$|\psi^{(h)}\rangle = |\text{vac}\rangle, \quad (15)$$

with energy $\varepsilon_h = 0$. The subspace with two particles on a site contains three states. For simplicity, we neglect the hybridization coupling γ and approximate the eigenstates with an additional particle by states with sharp occupations of the orbitals α ,

$$|\psi^{(p20)}\rangle = \frac{1}{\sqrt{2}} (\hat{b}_0^\dagger)^2 |\text{vac}\rangle, \quad (16)$$

$$|\psi^{(p11)}\rangle = \hat{b}_0^\dagger \hat{b}_1^\dagger |\text{vac}\rangle, \quad (17)$$

$$|\psi^{(p02)}\rangle = \frac{1}{\sqrt{2}} (\hat{b}_1^\dagger)^2 |\text{vac}\rangle, \quad (18)$$

with unperturbed energies $\varepsilon_{p20} = U_{00}$, $\varepsilon_{p11} = 2U_{01} + \delta$, and $\varepsilon_{p02} = 2U_{11} + 2\delta$.

Re-introducing the site index ℓ the unperturbed ground state reads

$$|\psi_0\rangle = \prod_{\ell} |\psi_{\ell}^{(0)}\rangle = \prod_{\ell} (a_0 \hat{b}_{0\ell}^\dagger + a_1 \hat{b}_{1\ell}^\dagger) |\text{vac}\rangle. \quad (19)$$

The correlation function between the neighboring sites 0 and 1 obtains a finite value in the first order of the perturbation expansion with respect to tunneling

$$\begin{aligned} \langle \psi | \hat{b}_{\alpha 0}^\dagger \hat{b}_{\alpha 1} | \psi \rangle &\simeq \langle \psi_0 | \hat{b}_{\alpha 0}^\dagger \hat{b}_{\alpha 1} | \psi_1 \rangle + \langle \psi_1 | \hat{b}_{\alpha 0}^\dagger \hat{b}_{\alpha 1} | \psi_0 \rangle \\ &= 2 \langle \psi_0 | \hat{b}_{\alpha 0}^\dagger \hat{b}_{\alpha 1} | \psi_1 \rangle. \end{aligned} \quad (20)$$

Here the relevant terms of the first-order state correction $|\psi_1\rangle$ possess an extra particle in one of the three possible

states on site 1 and a hole on site 0. These terms are related to the perturbation $-J_0\hat{b}_{01}^\dagger\hat{b}_{00}+J_1\hat{b}_{11}^\dagger\hat{b}_{10}$ and read

$$\left[\frac{a_0^2 J_0}{U_{00} - 2\varepsilon_0} (\hat{b}_{01}^\dagger)^2 - \frac{a_1^2 J_1}{U_{11} + 2\delta - 2\varepsilon_0} (\hat{b}_{11}^\dagger)^2 - \frac{a_0 a_1 (J_1 - J_0)}{U_{01} + \delta - 2\varepsilon_0} \hat{b}_{11}^\dagger \hat{b}_{01}^\dagger \right] \prod_{\ell \neq 0,1} (a_0 \hat{b}_0 + a_1 \hat{b}_1) |\text{vac}\rangle. \quad (21)$$

With this expression we obtain from Eqs. (20) and (14) that

$$\langle \hat{b}_{00}^\dagger \hat{b}_{01} \rangle \simeq \frac{2n_0}{U_{00}(2U_{01} + \delta - 2\varepsilon_0)} \left[2n_0 J_0 (2U_{01} + \delta - 2\varepsilon_0) - n_1 (J_1 - J_0) (U_{00} - 2\varepsilon_0) \right] \quad (22)$$

and

$$\langle \hat{b}_{10}^\dagger \hat{b}_{11} \rangle \simeq - \frac{2n_1}{(U_{11} + 2\delta - 2\varepsilon_0)(2U_{01} + \delta - 2\varepsilon_0)} \times \left[2n_1 J_1 (2U_{01} + \delta - 2\varepsilon_0) + n_0 (J_1 - J_0) (U_{11} + 2\delta - 2\varepsilon_0) \right]. \quad (23)$$

The transition from MI_{01} to MI_1 is related to $\langle \hat{b}_{00}^\dagger \hat{b}_{01} \rangle$ becoming negative. Approximating $2U_{01} + \delta - 2\varepsilon_0 \approx 2U_{01}$, which is consistent with our previous approximation to neglect γ on doubly occupied sites, the transition is expected to occur when

$$\frac{n_1}{n_0} \approx \frac{4J_0 U_{01}}{(J_1 - J_0) U_{00}} \quad (24)$$

or, equivalently, when

$$n_0 - n_1 \approx \frac{(J_1 - J_0) U_{00} - 4J_0 U_{01}}{(J_1 - J_0) U_{00} + 4J_0 U_{01}}. \quad (25)$$

* cstraeter@pks.mpg.de

† eckardt@pks.mpg.de

- [1] A. C. Hewson, *The Kondo problem to heavy fermions*, Vol. 2 (Cambridge university press, 1997).
- [2] P. Coleman, “Heavy fermions: Electrons at the edge of magnetism,” in *Handbook of Magnetism and Advanced Magnetic Materials* (John Wiley & Sons, Ltd, 2007).
- [3] Q. Si and F. Steglich, *Science* **329**, 1161 (2010).
- [4] M. Gulácsi, *Advances in Physics* **53**, 769 (2004).
- [5] I. Bloch, J. Dalibard, and W. Zwerger, *Rev. Mod. Phys.* **80**, 885 (2008).
- [6] M. Lewenstein, A. Sanpera, and V. Ahufinger, *Ultracold Atoms in Optical Lattices: Simulating quantum many-body systems* (Oxford University Press, Oxford (UK), 2012).
- [7] N. Gemelke, E. Sarajlic, Y. Bidel, S. Hong, and S. Chu, *Phys. Rev. Lett.* **95**, 170404 (2005).
- [8] T. Müller, S. Fölling, A. Widera, and I. Bloch, *Phys. Rev. Lett.* **99**, 200405 (2007).

- [9] C. Sias, A. Zenesini, H. Lignier, S. Wimberger, D. Ciampini, O. Morsch, and E. Arimondo, *Phys. Rev. Lett.* **98**, 120403 (2007).
- [10] G. Wirth, M. Ölschläger, and A. Hemmerich, *Nat. Phys.* **7**, 147 (2011).
- [11] M. Ölschläger, G. Wirth, and A. Hemmerich, *Phys. Rev. Lett.* **106**, 015302 (2011).
- [12] W. S. Bakr, P. M. Preiss, M. E. Tai, R. Ma, J. Simon, and M. Greiner, *Nature* **480**, 500 (2011).
- [13] C. V. Parker, L.-C. Ha, and C. Chin, *Nat. Phys.* **9**, 769 (2013).
- [14] S. Arlinghaus and M. Holthaus, *Phys. Rev. B* **84**, 054301 (2011).
- [15] S. Arlinghaus and M. Holthaus, *Phys. Rev. A* **85**, 063601 (2012).
- [16] T. Sowiński, *Phys. Rev. Lett.* **108**, 165301 (2012).
- [17] S.-L. Zhang and Q. Zhou, arXiv:1403.0210 (2014).
- [18] W. Zheng, B. Liu, J. Miao, C. Cin, and H. Zhai, arXiv:1402.4569 (2014).
- [19] S. Choudhury and E. J. Mueller, arXiv:1405.1398 (2014).
- [20] D. M. M Di Liberto, G. I. Japaridze, and C. M. Smith, arXiv:1405.4756 (2014).
- [21] J. Pietraszewicz, T. Sowiński, M. Brewczyk, J. Zakrzewski, M. Lewenstein, and M. Gajda, *Phys. Rev. A* **85**, 053638 (2012).
- [22] A. Isacson and S. M. Girvin, *Phys. Rev. A* **72**, 053604 (2005).
- [23] C. Wu, W. V. Liu, J. Moore, and S. D. Sarma, *Phys. Rev. Lett.* **97**, 190406 (2006).
- [24] C. Wu, *Phys. Rev. Lett.* **100**, 200406 (2008).
- [25] C. Wu, *Phys. Rev. Lett.* **101**, 186807 (2008).
- [26] X. Li, E. Zhao, and W. V. Liu, *Nat. Comm.* **4**, 1523 (2012).
- [27] X. Li, Z. Zhang, and W. V. Liu, *Phys. Rev. Lett.* **108**, 175302 (2012).
- [28] F. Pinheiro, G. M. Bruun, J.-P. Martikainen, and J. Larson, *Phys. Rev. Lett.* **111**, 205302 (2013).
- [29] J. Li, Y. Yu, A. M. Dudarev, and Q. Niu, *New J. Phys.* **8**, 154 (2006).
- [30] D.-S. Lühmann, K. Bongs, K. Sengstock, and D. Pfannkuche, *Phys. Rev. Lett.* **101**, 050402 (2008).
- [31] P.-I. Schneider, S. Grishkevich, and A. Saenz, *Phys. Rev. A* **80**, 013404.
- [32] H. P. Büchler, *Phys. Rev. Lett.* **104**, 090402 (2010).
- [33] K. R. A. Hazzard and E. Mueller, *Phys. Rev. A* **81**, 031602(R) (2010).
- [34] O. Dutta, A. Eckardt, P. Hauke, B. Malomed, and M. Lewenstein, *New J. Phys.* **13**, 023019 (2011).
- [35] M. Lacki and J. Zakrzewski, *Phys. Rev. Lett.* **110**, 065301 (2013).
- [36] O. Dutta, M. Gajda, P. Hauke, M. Lewenstein, D.-S. Lühmann, B. A. Malomed, T. Sowiński, and J. Zakrzewski, arXiv:1406.0181 (2014).
- [37] G. K. Campbell, J. Mun, M. Boyd, P. Medley, A. E. Leanhardt, L. G. Marcassa, D. E. Pritchard, and W. Ketterle, *Science* **313**, 649 (2006).
- [38] T. Best, S. Will, U. Schneider, L. Hackermüller, D. van Oosten, I. Bloch, and D.-S. Lühmann, *Phys. Rev. Lett.* **102**, 030408 (2009).
- [39] S. Will, T. Best, U. Schneider, L. Hackermüller, D.-S. Lühmann, and I. Bloch, *Nature* **465**, 197 (2010).
- [40] M. Mark, E. Haller, K. Lauber, J. Danzl, A. Daley, and H. Nägerl, *Phys. Rev. Lett.* **107**, 175301 (2011).

- [41] J. Heinze, S. Götze, J. Krauser, B. Hundt, N. Fläschner, D.-S. Lühmann, C. Becker, and K. Sengstock, *Phys. Rev. Lett.* **107**, 135303 (2011).
- [42] O. Jürgensen, F. Meinert, M. J. Mark, H.-C. Nägerl, and D.-S. Lühmann, *arXiv:1407.0835* (2014).
- [43] Since we consider a weak dimerization only, $V_1 < V_0$, we do not need to employ generalized Wannier orbitals, localized in the left and right minimum of each double well [Fig. 1(a)], as in B. Vaucher, S. R. Clark, U. Dörner, and D. Jaksch, *New J. Phys.* **9**, 221 (2007).
- [44] J. H. Shirley, *Phys. Rev.* **138**, B979 (1965).
- [45] H. Sambe, *Phys. Rev. A* **7**, 6 (1973).
- [46] A. Eckardt and M. Holthaus, *EPL* **80**, 50004 (2007).
- [47] A. Eckardt and M. Holthaus, *Phys. Rev. Lett.* **101**, 245302 (2008).
- [48] M. Wall and L. Carr, Open Source TEBD, <http://physics.mines.edu/downloads/software/tebd> (2009).
- [49] G. Vidal, *Phys. Rev. Lett.* **93**, 040502 (2004).
- [50] C. Honerkamp, *Phys. Rev. B* **68**, 104510 (2003).
- [51] C. Hotta and N. Furukawa, *Phys. Rev. B* **74**, 193107 (2006).
- [52] A. Eckardt, P. Hauke, P. Soltan-Panahi, C. Becker, K. Sengstock, and M. Lewenstein, *EPL* **89**, 10010 (2010).
- [53] J. Struck, C. Ölschläger, R. Le Targat, P. Soltan-Panahi, A. Eckardt, M. Lewenstein, P. Windpassinger, and K. Sengstock, *Science* **333**, 996 (2011).
- [54] S. Greschner, L. Santos, and T. Vekua, *Phys. Rev. A* **87**, 033609 (2013).
- [55] O. Tieleman, O. Dutta, M. Lewenstein, and A. Eckardt, *Phys. Rev. Lett.* **110**, 096405 (2013).
- [56] A. Dhar, T. Mishra, M. Maji, R. V. Pai, S. Mukerjee, and A. Paramekanti, *Phys. Rev. B* **87**, 174501 (2013).
- [57] D. Yudin, D. Hirschmeier, H. Hafermann, O. Eriksson, A. I. Lichtenstein, and M. I. Katsnelson, *Phys. Rev. Lett.* **112**, 070403 (2014).
- [58] N. Elstner and H. Monien, *Phys. Rev. B* **59**, 12184 (1999).
- [59] Experimentally n_0 and n_1 and the Fourier transforms of $n_0\chi_{00}^\ell$ and $n_1\chi_{11}^\ell$ can be measured via band mapping [8].
- [60] See supplemental material for the perturbative treatment of transitions within the MI phase..
- [61] R. Lim and M. V. Berry, *J. Phys. A: Math. Gen.* **24**, 3255 (1991).